Double ionization of helium by proton impact: A generalized-Sturmian approach

M. J. Ambrosio,[1,2,*] D. M. Mitnik,[1,2] L. U. Ancarani,[3] G. Gasaneo,[2,4] and E. L. Gaggioli[4]

[1]*Instituto de Astronomía y Física del Espacio (IAFE, CONICET–UBA), Casilla de Correo 67 - Sucursal 28 (C1428ZAA), Ciudad Autónoma de Buenos Aires, Argentina*

[2]*Consejo Nacional de Investigaciones Científicas y Técnicas, Buenos Aires, Argentina*

[3]*Théorie, Modélisation, Simulation, SRSMC, UMR CNRS 7565, Université de Lorraine, 57078 Metz, France*

[4]*Departamento de Física, Universidad Nacional del Sur, 8000 Bahía Blanca, Buenos Aires, Argentina*

(Received 1 September 2015; published 13 October 2015)

We present *ab initio* calculations for the double ionization of helium by fast proton impact, using the generalized-Sturmian-functions methodology and within a perturbative treatment of the projectile-target interaction. The cross-section information is extracted from the asymptotic behavior of the numerical three-body function that describes the emission process. Our goal is to provide benchmark first-order Born fully differential cross sections with which one may investigate the suitability of transition matrices calculated using approximate analytic-type solutions for the double continuum (the choice of effective charges or effective momenta to partially account for the internal target interactions being, to some extent, arbitrary). We also provide fully differential cross sections for the low-ejection-energy regime, which is beyond the suitable range of such perturbative methods. We find, however, that the effective momentum approach allows one to get at least a rough characterization of the most dominant physical process involved. We also compare our calculations with the only available relative experimental set, showing an agreement in shape that can be well understood within the given momentum transfer regime.

DOI: 10.1103/PhysRevA.92.042704 PACS number(s): 34.50.Fa, 31.15.A−

I. INTRODUCTION

The double ionization of helium by charged-particle impact constitutes an intricate four-body Coulomb problem, appreciably more complex than in the case of impact by photons. This is due to the, in principle, two-center interaction between the projectile and the target. If the projectile is positively charged, the collision can lead to the capture of one of the target electrons and the ionization of the other one. However, this process is several orders of magnitude less probable than ordinary single or double ionization (DI), particularly for projectiles on the order of 1–10 MeV/amu [1]. In this contribution we focus on proton-impact ionization of helium within the high-incident-energy regime for which the capture process can be disregarded. The most basic mechanisms which produce DI, called shake-off (SO), two-step-1 (TS1) and two-step-2 (TS2) [2], were studied with approximate descriptions of both the helium ground state and the double continuum [3,4]. The TS1 process implies a collision between the projectile and one of the target electrons, which subsequently impacts the other one, and both end up being ejected to the continuum. In the TS2 mechanism, the projectile hits the two target electrons successively and kicks them out of their parent core. Another mechanism, called two-step-1-elastic (TS1EL) in Ref. [3], contemplates a further collision between the projectile and the electron ejected via the electron-electron interaction after the first impact. Processes TS2 and TS1EL require two projectile-target Born interactions.

The majority of previous works, both theoretical and experimental, discussed integrated cross sections [5–10]. To a lesser extent, fully differential cross sections (FDCS), which provide the most detailed information of the double-ionization process, have also been investigated experimentally and theoretically [3,4,11,12]. For the case of electron impact several FDCS measurements under different emission energies and momentum transfer regimes have been carried out by the Orsay and Heidelberg groups (restricted to fast projectiles; see Refs. [13–16]); many theoretical studies have been dedicated to interpreting these data (a nonexhaustive list of references is given in the introduction of our most recent publications [17,18] on the topic). In comparison, much less frequent are differential cross-section measurements for proton impact. The one reported by Fischer *et al.* [11] is the only experimental data set that provides a fully differential cross section, while previous works [5–8] have measured total cross sections and double-to-single ionization ratios. In Ref. [11], the authors report that one week was required to observe 200 000 double-ionization events, enough to produce FDCS. A set of multiply, but not fully, differential cross-section measurements, along with their theoretical counterparts, was published in Ref. [3] for double ionization of helium by very fast (6 MeV) protons, in addition to a comparison of their calculations with one of the kinematic configurations from Ref. [11].

On the theoretical side, the collision of charged projectiles with helium atoms constitutes a full four-body problem which poses a formidable challenge. If the projectile is fast enough, its interaction with the target can be considered a perturbation, with the projectile experiencing a single deflection. While the resulting three-body problem is still challenging enough, there exists nowadays a variety of numerical schemes that can solve it from first principles in a time-dependent [9,10] or time-independent fashion [19–22]. Other approaches use approximate analytical three-body functions, mostly based on the 3C (also named C3 or BBK) wave function [23,24] which is asymptotically correct when all three particles are far from each other. Quite a number of variants of the 3C function have

*Corresponding author: mj_ambrosio@iafe.uba.ar

been proposed in the literature; they all aim to improve the 3C function by including extra physical information, thereby extending its range of validity. One way to achieve this is by introducing effective charges which, although with some restrictions, are largely arbitrary. Effective charges allow one to better account for intratarget interactions as well as projectile-target ones beyond the first Born approximation (FBA). The comparison of calculated cross sections, in particular FDCS, with either experimental or benchmark *ab initio* theoretical data then provides an instrument to point out which set is more physically sound for given kinematical conditions. While such approximate analytical three-body functions generally provide only qualitative descriptions, they are often good enough to analyze and identify the dominant collisional mechanisms. Fully numerical approaches, in turn, provide, in principle, exact solutions, but the interpretation of the resulting cross sections is less straightforward. One has to infer which mechanics come into play just by analyzing the cross sections.

For the double ionization of helium by electron impact, thorough comparisons between theoretical and experimental FDCS, on the one hand, and between fully numerical and approximate analytical calculations, on the other hand, have been presented in the literature (see, e.g., the recent studies in Refs. [17,18] and references therein). In contrast, very little has been done for proton impact. This paper aims to contribute to filling that gap.

We calculate FDCS with a Sturmian approach based on generalized Sturmian functions (GSF) [22,25]. The spectral method has been shown to deal successfully with three-body scattering problems, as illustrated recently through the study of the double ionization of helium by photons [26] or by fast electrons [17,18]. The GSF method can generate both the target bound state and its scattering function with, in principle, arbitrary numerical accuracy. Here, we apply it to study the fast proton-helium double-ionization process: in chosen kinematical conditions we provide, within the FBA, benchmark FDCS with three goals in mind. First, we want to compare our FDCS with those presented in the recent theoretical investigations based on perturbative methods using approximate analytical three-body wave functions [4,12]. Second, we wish to identify the collisional processes and contrast them with those of the better-known electron-impact counterpart. Third, we want to find out if a fully numerical treatment within the FBA is able to reproduce the main features observed in the experiments reported in [11].

López *et al.* [12] made a thorough investigation of fast proton-helium FDCS under a variety of kinematical conditions. They demonstrated a great degree of variation in the calculated cross sections when using different analytical final-state continuum functions (3C and variants including effective charges). They also showed that the target bound-state description affects the FDCS palpably. The same authors further tackled the problem with an approach involving effective momenta [4]. In this second study, the obtained cross sections present structures that vary slowly with the ejection angles, a trend, to some degree, analogous to that observed for electron impact [16,18,27]. By providing FDCS with our GSF method, we wish to evaluate the success of these perturbative schemes.

Recall that the 3C continuum function is valid when the particles are moving away from each other quickly and/or are far apart. There is therefore a particular niche for which the perturbative methods are not well suited: low emission energies. To explore this regime, we have performed GSF calculations considering a total excess energy of 6 eV, with the equal-energy-sharing case, $(3+3)$ eV, as well as the unequal configuration, $(1.5+4.5)$ eV. The purpose here is twofold. First, we explore these kinematical conditions with a reliable method to establish the physical processes that come into play when the two electrons are emitted very slowly. Second, our benchmark results can be used to test the quality of effective charges intended to extend the validity of the 3C function to the low-energy domain. By no means do we intend to disqualify the perturbative approaches. On the contrary, we regard them as complementary to *ab initio* methods, each exploring adequately different kinematical ranges.

Since there is a lot of variation, even within the first-order Born model, from one perturbative model to the next, we are not considering in the present work any second-order Born interactions of the projectile with the target atom. An interested reader can find second-order studies in Refs. [3,28,29]. For this contribution we consider it a priority to establish first the first-order Born ground properly. To this order, valid for fast projectiles, the phenomenon of electronic capture is not incorporated in the calculations, either numerical or perturbative. Thus, only the effects of the well-known two-step-1 and shake-off mechanisms are expected to be observed in the calculated FDCS.

The rest of the paper is arranged as follows. In Sec. II we begin by outlining the theoretical framework on which our calculations are based. Section III, dedicated to the results, is divided in three subsections. The first one is devoted to a comparison of the GSF results with those obtained with the effective charges and effective momenta approaches [4,12]. Section III B contains the studies performed in the low-emission regimes (6 eV excess energy): we make a comparison with a preexisting result [4] in equal energy sharing; we then increase the momentum transfer to observe more prominent nondipolar effects. In Sec. III C we contrast our numerical calculations with the experimental data reported in [11]. Finally, a brief summary is provided in Sec. IV.

Atomic units ($\hbar = e = m_e = 1$) are used throughout the article, unless otherwise stated.

II. FAST PROJECTILE FORMULATION AND GSF APPROACH

Our treatment of the four–body scattering problem is based on a perturbative series of the projectile-target interaction, kept up to the first order. The resulting three-body problem is then solved with the GSF method.

Let $\mathbf{r}_1$ denote the position of the projectile (mass m_P), $\mathbf{r}_i$ $(i = 2,3)$ denote that of the two helium electrons with respect to its nucleus (mass m_T, charge $Z = 2$), and $r_{ij} = |\mathbf{r_i} - \mathbf{r_j}|$ denote the distance between particles i and j. The full four-body Hamiltonian reads

$$H = -\frac{1}{2\mu_{TP}}\nabla_1^2 - \frac{1}{2\mu_T}\nabla_2^2 - \frac{1}{2\mu_T}\nabla_3^2 + \frac{Z}{r_1} - \frac{1}{r_{12}} - \frac{1}{r_{13}} - \frac{Z}{r_2} - \frac{Z}{r_3} + \frac{1}{r_{23}}, \quad (1)$$

with the reduced masses defined as $\mu_{TP} = \frac{m_P m_T}{m_P+m_T}$ and $\mu_T = \frac{m_T}{m_T+1}$. Similar to Refs. [18,30], we write subsequently

$$H_0 = h_p + h_{He}, \tag{2}$$

where

$$h_{He} = \left(-\frac{1}{2\mu_T}\nabla_2^2 - \frac{1}{2\mu_T}\nabla_3^2 - \frac{Z}{r_2} - \frac{Z}{r_3} + \frac{1}{r_{23}}\right) \tag{3}$$

is the three-body helium Hamiltonian and $h_p = -\frac{1}{2\mu_{TP}}\nabla_1^2$ is the free-particle kinetic term associated with the projectile. The two Hamiltonians in (2) act separately on the subsystem (2,3) and (1). They are coupled through the perturbation

$$\bar{W} = \frac{Z}{r_1} - \frac{1}{r_{12}} - \frac{1}{r_{13}}. \tag{4}$$

The four-body Hamiltonian is then

$$H = H_0 + \bar{W}, \tag{5}$$

and the Schrödinger equation with outgoing-type (+) behavior reads

$$[H_0 + \bar{W} - E]\Psi^+(\mathbf{r}_1,\mathbf{r}_2,\mathbf{r}_3) = 0, \tag{6}$$

where E is the total energy.

As shown in Ref. [30], the Schrödinger equation (6) can be transformed into a system of coupled differential equations if the solution is proposed as

$$\Psi^+(\mathbf{r}_1,\mathbf{r}_2,\mathbf{r}_3) = \sum_n \Psi^{(n)+}(\mathbf{r}_1,\mathbf{r}_2,\mathbf{r}_3), \tag{7}$$

where each order retains n interactions $\bar{W}$ between the projectile and the target. Allowing for only one interaction, we need the zeroth- and first-order expressions, which read

$$[H_0 - E]\Psi^{(0)+}(\mathbf{r}_1,\mathbf{r}_2,\mathbf{r}_3) = 0, \tag{8a}$$

$$[H_0 - E]\Psi^{(1)+}(\mathbf{r}_1,\mathbf{r}_2,\mathbf{r}_3) = -\bar{W}\Psi^{(0)+}(\mathbf{r}_1,\mathbf{r}_2,\mathbf{r}_3). \tag{8b}$$

The zeroth order corresponds to a separable solution, $e^{i\mathbf{k}_i\cdot\mathbf{r}_1}\Phi_i(\mathbf{r}_2,\mathbf{r}_3)$, where $\Phi_i(\mathbf{r}_2,\mathbf{r}_3)$ is the two-electron helium ground state and the fast incident projectile is described by a plane wave of momentum $\mathbf{k}_i$. The first-order solution, verifying Eq. (8b), is written as [30]

$$\Psi^{(1)+}(\mathbf{r}_1,\mathbf{r}_2,\mathbf{r}_3) = \frac{1}{(2\pi)^{3/2}}\int d\mathbf{k} e^{i\mathbf{k}\cdot\mathbf{r}_1}\Phi_{sc}^+(\mathbf{k},\mathbf{r}_2,\mathbf{r}_3), \tag{9}$$

where the three-body scattering (labeled sc) function Φ_{sc}^+ characterizes the physics of the ejected electrons. Let E_a denote the energy of two electrons interacting with the nucleus in the final state and $k^2/2$ be the energy associated with the projectile: the total energy of the system is then $E = E_a + k^2/(2\mu_{TP})$. Let the projectile be scattered with momentum $\mathbf{k}_f$, and define the momentum transfer vector $\mathbf{q} = \mathbf{k}_i - \mathbf{k}_f$. Inserting Eq. (9) into (8b), we obtain a driven equation for $\Phi_{sc}^+(\mathbf{q},\mathbf{r}_2,\mathbf{r}_3)$ [30]:

$$[h_{He} - E_a]\Phi_{sc}^+(\mathbf{q},\mathbf{r}_2,\mathbf{r}_3) = -\frac{4\pi}{q^2}\frac{1}{(2\pi)^3}(Z - e^{i\mathbf{q}\cdot\mathbf{r}_2} - e^{i\mathbf{q}\cdot\mathbf{r}_3}) \times \Phi_i(\mathbf{r}_2,\mathbf{r}_3), \tag{10}$$

where we have made explicit the $\mathbf{q}$ dependence in the three-body scattering wave function.

Formally, we can write the asymptotic behavior of $\Phi_{sc}^+(\mathbf{q},\mathbf{r}_2,\mathbf{r}_3)$ as [31]

$$\Phi_{sc}^+(\mathbf{q},\mathbf{r}_2,\mathbf{r}_3) \underset{\rho\to\infty}{\longrightarrow} (2\pi i)^{1/2}\kappa^{\frac{3}{2}}T_{\tilde{\mathbf{k}}_2,\tilde{\mathbf{k}}_3}\frac{e^{i[\kappa\rho-\lambda_0\ln(2\kappa\rho)-\sigma_0]}}{\rho^{\frac{5}{2}}}, \tag{11}$$

where $\rho = \sqrt{r_2^2 + r_3^2}$ is the hyperradius, $\kappa = \sqrt{2E_a}$ the hypermomentum, σ_0 is a Coulomb phase, and λ_0 is a hyperangle-dependent asymptotic Sommerfeld parameter. The transition matrix $T_{\tilde{\mathbf{k}}_2,\tilde{\mathbf{k}}_3}$ that is built into the scattering solution can equivalently be defined as

$$T_{\tilde{\mathbf{k}}_2,\tilde{\mathbf{k}}_3} = \frac{4\pi}{q^2}\frac{1}{(2\pi)^3} \times \left\langle\Psi^-_{\tilde{\mathbf{k}}_2,\tilde{\mathbf{k}}_3}(\mathbf{r}_2,\mathbf{r}_3)\right| - Z + e^{i\mathbf{q}\cdot\mathbf{r}_2} + e^{i\mathbf{q}\cdot\mathbf{r}_3}\left|\Phi_i(\mathbf{r}_2,\mathbf{r}_3)\right\rangle, \tag{12}$$

which provides the more familiar expression used in the FBA. In our framework, the transition matrix is extracted from $\Phi_{sc}^+(\mathbf{q},\mathbf{r}_2,\mathbf{r}_3)$, not from Eq. (12).

For two electrons escaping with energies E_2 and E_3 in the solid angles $d\Omega_2$ and $d\Omega_3$, the FDCS, within the FBA, is defined as

$$\frac{d^5\sigma}{d\Omega_2 d\Omega_3 d\Omega_f dE_2 dE_3} = (2\pi)^4\frac{k_f k_2 k_3}{k_i}\left|T_{\tilde{\mathbf{k}}_2,\tilde{\mathbf{k}}_3}\right|^2, \tag{13}$$

where the projectile, whose energy $E_f = k_f^2/(2\mu_{TP})$ is determined by total-energy conservation, is scattered in the solid angle $d\Omega_f$. This definition allows for a direct comparison with experimental data. In order to compare our results with the theoretical results presented in Ref. [4,12], on the other hand, we shall also use the alternative, but equivalent, definition of the cross section

$$\frac{d\sigma}{d\mathbf{k}_2 d\mathbf{k}_3 d\mathbf{q}_\perp} = \frac{(2\pi)^4}{v_p^2}\left|T_{\tilde{\mathbf{k}}_2,\tilde{\mathbf{k}}_3}\right|^2, \tag{14}$$

which is differential with respect to the ejected electrons' momenta and the transverse momentum transfer $\mathbf{q}_\perp$ (the perpendicular component of $\mathbf{q}$ with respect to the beam axis); v_p is the velocity of the incident projectile.

We use the GSF method to solve the driven equation for a given $\mathbf{q}$. For convenience, as explained in [17,18], the helium ground state is also constructed within the GSF formalism. GSF basis sets with negative energy were shown to be very efficient in obtaining two-electron bound states [22,32,33]. In order to calculate the scattering function, we proceed as outlined in Ref. [18]: $\Phi_{sc}^+(\mathbf{q},\mathbf{r}_2,\mathbf{r}_3)$ is decomposed in total-angular-momentum partial waves and subsequently expanded in a Sturmian basis [see Eq. (19) of [18]]; this converts Eq. (10) into a linear system [similar to Eq. (21) of [18]] which is solved with standard methods. In all kinematical configurations considered below, convergence with respect to the number of partial waves has been verified. From $|\Phi_{sc}^+(\mathbf{q},\mathbf{r}_2,\mathbf{r}_3)|$ at large enough ρ (50 a.u. for 20 eV excess energy and 120 a.u. for the low-energy configurations, 6 eV excess energy) we extract $|T_{\tilde{\mathbf{k}}_2,\tilde{\mathbf{k}}_3}|$ using Eq. (11) and, finally, the FDCS through either expression (13) or (14).

III. RESULTS

We arrange the results in three subsections. First, we compare our cross sections with the dynamically screened 3C (hereinafter DS3C) and effective momenta 3C (hereinafter EM3C) results presented by López and coworkers [4,12]. The objective is twofold: (i) to evaluate which of the two analytic proposals is more appropriate and (ii) to provide results that can be used for numerical reference to test further perturbative models. We then explore the double-ionization dynamics for slow emitted electrons for both equal and unequal energy sharing and compare the outcome with the EM3C results. In this energy range, perturbative approaches are not appropriate but ours is, and we expect to explore the dominant processes within it. In the last subsection we compare our theoretical FDCS with available experimental data of Fischer *et al.* [11].

Only coplanar configurations are considered, and all angles are defined with respect to the incident-beam direction. The cross sections will be presented as contour plots in θ_2 and θ_3, with the intensity scale indicated on the right-hand side.

A. Comparison: GSF, DS3C, and EM3C

In order to compare our results with the work of López *et al.* [4,12], we consider here the double ionization of helium by protons impinging with an energy of 700 keV. Even in a first-order Born calculation, the use of effective charges allowed them to distinguish between positively and negatively charged projectiles. In our strictly FBA, no distinction can be made about the sign of the projectile. In Ref. [12], the authors presented, in a number of contour plots (and some selected cuts), the FDCS defined by Eq. (14). They showed that the results (shapes and magnitudes) are widely affected, on the one hand, by the representation of the initial target state and, on the other hand, by the effective charges chosen for the postcollisional dynamics.

Concerning the helium ground state employed, the one used in [4,12] and ours differ significantly. The authors of [12] use two types of Bonham and Kohl bound-state functions: a simple, two-parameter (type-7) function (called GS1) and a more refined, modified-type-9 one, with five parameters (called GS2). These trial functions yield bound energies of -2.8756 and -2.9019 a.u., respectively. In our formulation, the helium ground state is obtained with the GSF method [32,33], with an energy of -2.9033 a.u., using 20 Sturmians per coordinate per partial wave, with individual angular momenta up to 4. In this paper we shall compare our cross-section results only with those of [4,12] that employ the GS2 ground state.

Since the main purpose of this contribution is to compare the descriptions of the continuum functions, in order to discard any initial-state-related issue, we have also considered a helium ground state of poorer quality, with an energy close to the GS2 counterpart (using as few as 5 Sturmians per partial wave per coordinate and keeping the same angular momentum values, we achieved a ground-state energy of -2.9024 a.u.). Both calculated FDCS presented no appreciable differences; therefore, we may consider that any discrepancy between the results of López *et al.* and ours is to be attributed essentially to the continuum functions.

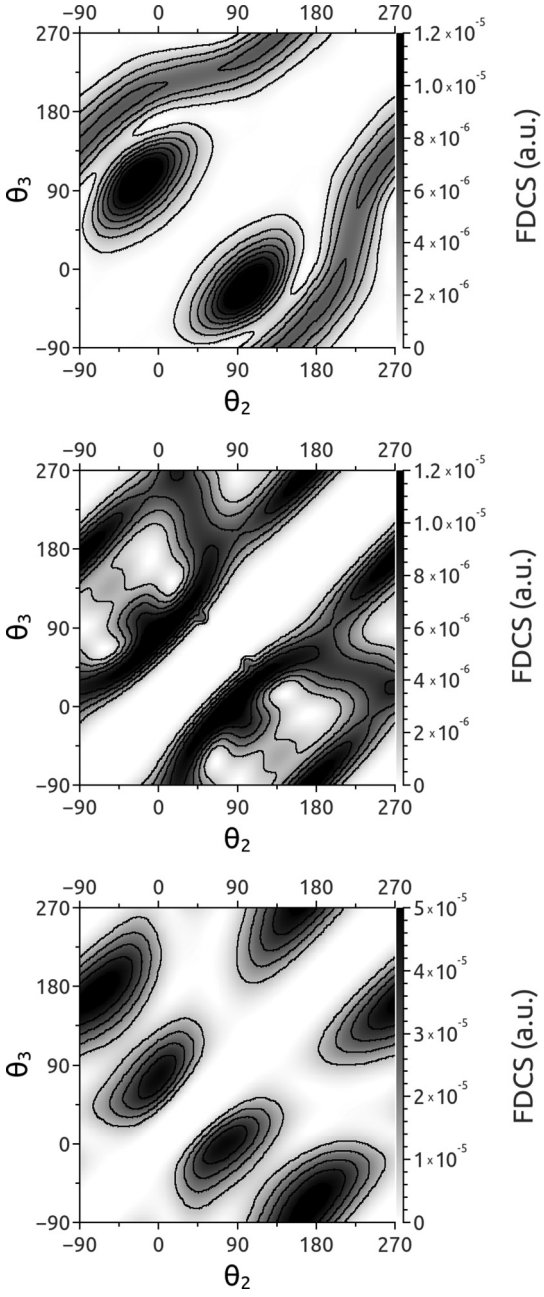

FIG. 1. Fully differential cross section for helium double ionization by proton impinging at 700 keV. The two emitted electrons each take 10 eV, and the proton transfers to the atomic system a momentum $q = 0.9$ a.u., oriented at $\theta_q = 40.18^\circ$. (top) Present GSF, (middle) DS3C [12], and (bottom) EM3C [4].

We start with the case in which the two electrons are ejected in the scattering plane in directions θ_2 and θ_3 with equal energy: $E_2 = E_3 = 10$ eV. This corresponds to a momentum transfer of modulus $q = 0.9$ a.u. oriented at $\theta_q = 40.18^\circ$. A comparison of results is presented by the contour plots in Fig. 1. The structures we obtain with the GSF method (top panel) differ substantially from the DS3C results [12] (middle panel). The GSF results vary less rapidly with the ejection angles. At the same time, the DS3C structures are more extended, in the sense that there is no clear frontier between the recoil

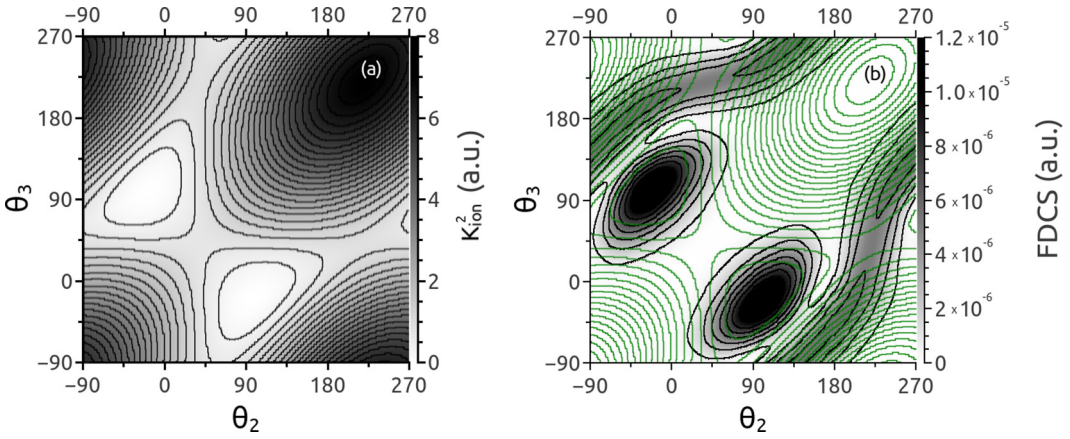

FIG. 2. (Color online) (a) Squared modulus of the momentum transferred to the helium nucleus $K^2_{\rm ion}$. Both electrons emerge equally sharing the 20 eV excess energy, $q = 0.9$ and $\theta_q = 40.18^\circ$ with respect to the incident direction. (b) GSF FDCS for these kinematical conditions, with the $K^2_{\rm ion}$ contours superimposed [in green (gray)].

and the binary peaks. Less profound are the differences found between the GSF and the EM3C [4] results (bottom panel). They both present a smoother angular dependence but differ in key features such as the recoil-structure shape and the relative heights of each peak.

We should add here that, in the case of electron impact, in contrast to the 3C counterpart, *ab initio* calculations such as the convergent close coupling (CCC) [27] showed a more prominent binary peak. In the present proton case, the comparison between our numerical results and those of the 3C variants reveals a similar feature.

There is also a subtle difference between the GSF result and the 3C-based cross sections. As can be observed when visually comparing Fig. 1 (top panel) with Fig. 2, the binary peak location in the GSF case coincides exactly with a configuration of minimum momentum transfer to the He^{++} core, $\mathbf{K}_{\rm ion} = \mathbf{q} - \mathbf{k}_2 - \mathbf{k}_3$. The peak is slightly displaced in the DS3C and EM3C cross sections. Moreover, the DS3C model binary peak occurs when the electrons are emitted at exactly right angles. In our GSF calculation the binary peak appears for electrons emitted at mutual angles that are wider than 90°, a feature readily explained by the interelectronic repulsion forcing the fragments farther apart in coplanar geometry (the same was also observed in other fully numerical results [16,27] for double ionization by electron impact).

As a second comparison, consider now the same projectile energy (700 keV), the same momentum transfer ($q = 0.9$ a.u.), and the same excess energy (20 eV) but unequal energy sharing: $E_2 = 5$ eV and $E_3 = 15$ eV. Our GSF and the DS3C results of [12] are compared in Fig. 3. The binary peaks are the most dominant features present in the GSF FDCS for the unequal-energy example [see Fig. 3(a)]. The DS3C scheme, in turn, appears to underestimate them (relative to the binary and back-to-back structures), as shown in Fig. 3(b). The DS3C approach presents back-to-back emission with the faster electron ejected in the directions parallel or antiparallel to the momentum transfer. Both situations are depicted as equally likely in the DS3C FDCS. This is not the case in the GSF result: only the emission of the faster electron in the direction opposite to the momentum transfer is important [see Fig. 3(a)].

The first likely candidate responsible for the back-to-back structures, particularly with the fast electron emitted parallel to **q**, would be the shake-off mechanism. However, Dorn *et al.* [34] ruled it out as a viable option to produce this emission. They stated that the fast electron would have to be ejected

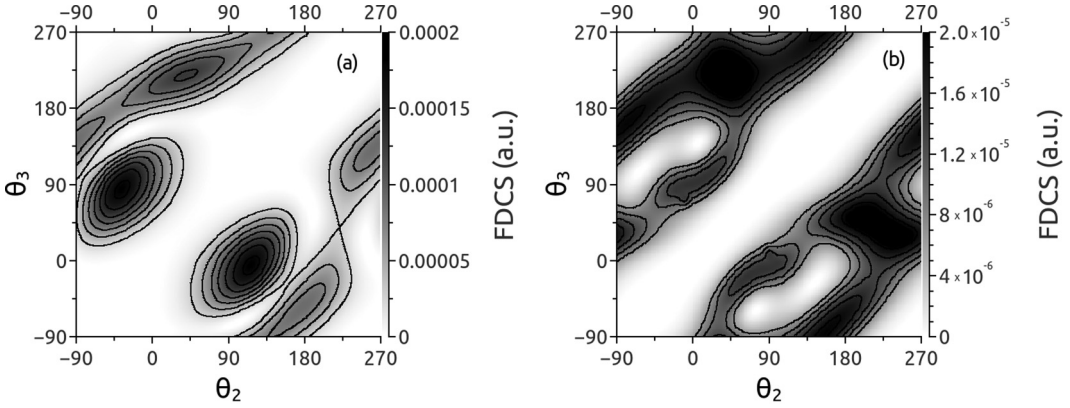

FIG. 3. Fully differential cross section for helium double ionization by protons impinging at 700 keV and transferring to the atomic system a momentum $q = 0.9$ a.u., oriented at $\theta_q = 40.18^\circ$. The two electrons are ejected with unequal energy sharing: $E_2 = 5$ eV, $E_3 = 15$ eV. (a) Present GSF and (b) DS3C [12].

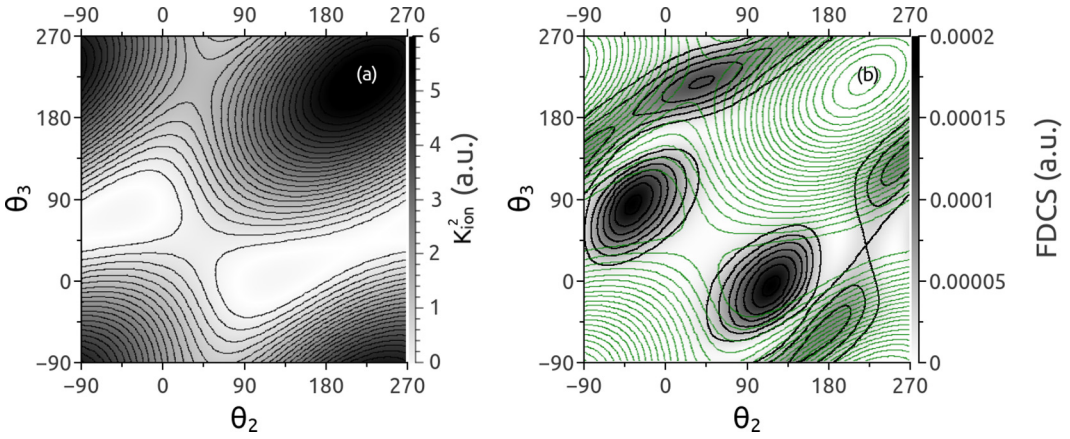

FIG. 4. (Color online) (a) Squared modulus of the momentum transferred to the nucleus $K^2_{\rm ion}$. (b) Same as Fig. 3(a), but superimposing the contours in (a) [in green (gray)].

with a higher velocity so that the effective charge change felt by the slow electron can be nonadiabatic. Therefore, for the energy sharing considered in this contribution, the mechanism can be disregarded. To explain the back-to-back peaks we are left with more abrupt mechanisms, involving pure collisions, and not soft relaxations to the continuum.

We now are going to briefly justify that the back-to-back emission, in our first-order Born context, should be dominant only when the fast electron leaves in the $-\mathbf{q}$ direction and weaker when it goes along $\mathbf{q}$. The occurrence is partly explained by Fig. 4. In Fig. 4(b) we show the GSF cross section superimposed with the contour plot of the squared modulus of the momentum transferred to the residual core [Fig. 4(a)]. After one of the electrons acquires the momentum provided by the projectile, the final back-to-back configuration requires at least one interaction with the nucleus; if that were not the case, there would be no electron (either of them) in the $-\mathbf{q}$ direction (indeed, a head-on collision of two bodies with equal mass would imply that they simply *swap* their respective momenta). The interaction with the core should transfer some momentum to the nucleus, with a magnitude of the order of the momentum of the electrons (i.e., on the order of 1). However, the final configuration with the fast electron parallel to $\mathbf{q}$ gives nearly no momentum transfer to the nucleus and therefore is an unlikely process. The exactly opposite scenario does incorporate an appreciable amount of momentum transferred to the core, denoting further intratarget interactions, and therefore cannot be ruled out. The above does not agree with the CCC (theoretical) FDCS presented in the work by Dorn *et al.* [34].

In contrast to the recoil and back-to-back structures, the binary ones do not require significant participation of the nucleus and therefore can exist in the (θ_2,θ_3) directions which imply almost no momentum acquired by the parent core [see Fig. 4(b)].

A second argument at play in the back-to-back phenomenon in Fig. 3 comes from the analysis of the driven term in Eq. (10). Retaining the dipolar term in the exponentials, we have

$$(Z - e^{i\mathbf{q}\cdot\mathbf{r}_2} - e^{i\mathbf{q}\cdot\mathbf{r}_3}) \approx -i(\mathbf{q}\cdot\mathbf{r}_2 + \mathbf{q}\cdot\mathbf{r}_3) = -i\frac{\rho}{\kappa}\mathbf{q}\cdot(\tilde{\mathbf{k}}_2 + \tilde{\mathbf{k}}_3), \qquad (15)$$

where in the second approximation we used the position-dependent momenta $\tilde{\mathbf{k}}_j = \frac{\kappa}{\rho}\mathbf{r}_j$ $(j = 2,3)$, defined originally in [35] and more explicitly in [31]. In our formulation, it is the driven term that dictates how a particular geometrical configuration is enhanced or suppressed (see [18]). We thus plot in Figs. 5(a) and 5(b) the magnitude $|\hat{\mathbf{q}}\cdot(\tilde{\mathbf{k}}_2 + \tilde{\mathbf{k}}_3)|$ and a superimposition with the FDCS, respectively. This comparison is in line with the electron-impact analysis presented by

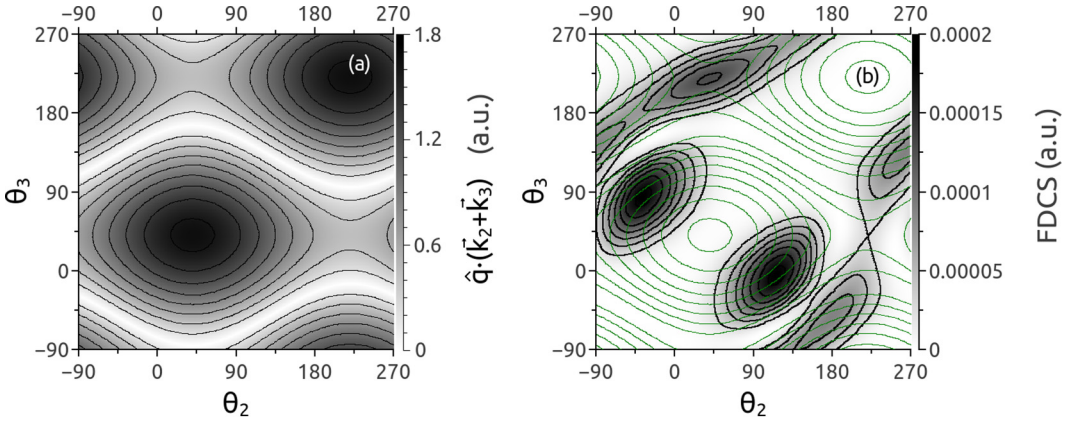

FIG. 5. (Color online) (a) $|\hat{\mathbf{q}}\cdot(\tilde{\mathbf{k}}_2 + \tilde{\mathbf{k}}_3)|$. (b) Same as Fig. 3(a), but superimposing the contours in (a) [in green (gray)].

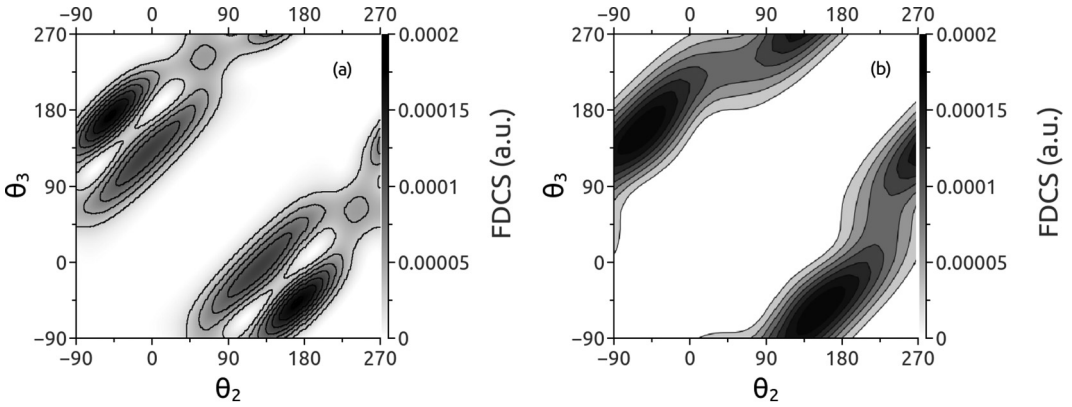

FIG. 6. Fully differential cross section for helium double ionization by protons impinging at 700 keV and transferring to the atomic system a momentum $q = 0.9$ a.u., oriented at $\theta_q = 40.18^\circ$. The two ejected electrons both have 3 eV. (a) Present GSF and (b) EM3C [4].

Lahmam-Bennani *et al.* [14], who related the dips in the FDCS considering the conditions that nullify Eq. (15).

The introduction of effective charges into the 3C function is a means to account for the interactions between the target components as well as the projectile with the target subsystem. The charges affect very strongly the shapes and magnitudes of the corresponding FDCS, as can be seen in the systematic 3C versus DS3C comparison in [12]. The dynamical screening corrects the 3C overestimation of the back-to-back emission but introduces rapidly varying structures that cannot be reproduced in our *ab initio* calculation. Thus, we infer that the use of such approximate analytical three-body functions leads to results that are not without shortcomings. We should add that there exists a large variety of effective-charge proposals, and there is not a clear way to choose which one is the appropriate. So it is difficult to be certain about the correctness of the obtained results.

B. Low-ejected-energy regime

We now consider the regime of two electrons ejected at lower energies. The application of distorted-wave methods to this emission regime can be seen as an overreach, but nonetheless, we will see that the EM3C approach can manage to describe some key FDCS features. In Ref. [4] the authors evaluated the double ionization of helium by proton (and antiproton) impact, ejecting the electrons at slow velocities. Their equal emission energies are 3 eV, with $q = 0.9$ a.u. oriented at $\theta_q = 40.18^\circ$ and an incident energy of 700 keV for the protonic projectiles. Our exact treatment of the two-electron continuum enables us to explore confidently this low-energy situation and provides insight that is complementary to that performed by López and coworkers using distorted-wave methods. In Fig. 6 we compare our GSF result with the EM3C one [4]. Both approaches indicate a recoil peak more relevant than the binary one. This can be understood since the electrons acquire small velocities after the collision and they may interact one further time with the core. The classical picture corresponds to an orbit around the nucleus before the electron is finally released.

While the EM3C results suggest a disappearance of the binary peak, the same is not observed in our GSF FDCS, which presents a diminished but still present binary peak. Although not exactly matching our *ab initio* results, the EM3C manages to give a qualitative agreement that reflects the most significant cross-section structure, namely, the recoil peak. This is a strong hint that the effective momentum approach makes possible the application of distorted-wave approximations within energy ranges that would normally be regarded as inappropriate.

Still within the low-ejected-energy regime, another kinematical condition was considered: a momentum transfer above unity to allow for more nondipolar effects: $q = 1.25$ a.u., oriented at $\theta_q = 61.82^\circ$, with a projectile energy maintained at 700 keV with an excess energy of 6 eV. Equal- and unequal-energy-sharing conditions are studied, with both electrons emitted with 3 eV or (1.5 + 4.5) eV. The amount of momentum transfer to the target would indicate some expected back-to-back emission. This is indeed confirmed by observing both equal- and unequal-energy-sharing configurations in Fig. 7, with the effect being more dominant in the latter.

For the equal-energy-sharing scenario [Fig. 7(a)] we have again recoil structures which are higher than the binary ones. In comparison to Fig. 6, the main differences that emerge are the slightly more pronounced back-to-back emission and a stronger binary peak.

The unequal-energy case, as in Sec. III A, shows back-to-back emission when the fast electron goes against the direction of the momentum transfer. The slower electron is pushed preferentially in the **q** direction, with their mutual repulsion serving as a guide. Under this particular kinematical condition, there is a large amount of momentum transferred to the target, yet the electrons leave with slow velocities. Therefore, the core has to absorb a portion of that transferred momentum in most emission geometries. Regarding the back-to-back ejection, we observe the same result as in the previous section: it is more likely to have the fast electron sent in the $-\mathbf{q}$ direction. Both arguments apply, but in the present case the dipolar terms of the exponential yield a near-zero value that is nearly replicated in the FDCS; Fig. 8 shows a comparison similar to that in Fig. 5.

As can be expected, recoil and binary peaks imply ejections at narrower mutual angles when the energy is shared evenly. This configuration maximizes the velocity magnitude sum and roughly implies that the electrons have less interaction time to push each other apart.

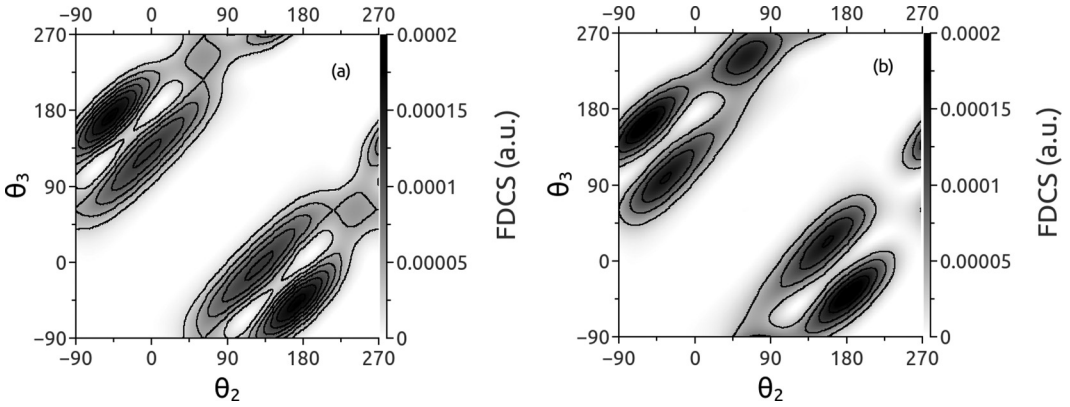

FIG. 7. GSF fully differential cross section for helium double ionization by protons impinging at 700 keV and transferring to the atomic system a momentum $q = 1.25$ a.u., oriented at $\theta_q = 61.82^\circ$. The excess energy E_a is 6 eV. (a) Equal energy sharing $E_2 = E_3 = 3$ eV. (b) Unequal energy sharing, $E_2 = 1.5$ eV, $E_3 = 4.5$ eV.

C. Comparison with experimental data

So far, we have looked at several physical aspects, comparing our GSF results with those of López and collaborators. In this section we compare our calculations with the data set (relative scale) measured by Fischer *et al.* [11]. In their experiment, the incident proton has an energy of 6 MeV, considerably faster than those studied in the previous sections. Due to the low experimental counting rate, the measurements were made with the collection of electrons with $E_2 = E_3 <$ 25 eV and momentum transfers ranging in magnitude q from 1.4 to 2.0 a.u and in angle θ_q from 75° to 85°. This range of variation for the quantities $E_2, E_3, \mathbf{q}$ implies that the label *fully differential* applies loosely for the measured cross sections. The most critical variable is the variation of q since the FDCS inherits an explicit factor $1/q^4$. Therefore, we considered an average q value using the following expression:

$$\langle q \rangle = \left[\frac{1}{q_{\max} - q_{\min}} \int_{q_{\min}}^{q_{\max}} \frac{1}{q^4} dq \right]^{-1/4}, \qquad (16)$$

which for $q_{\min} = 1.4$ a.u. and $q_{\max} = 2.0$ a.u. yields $\langle q \rangle = 1.656$ a.u. For the direction of the momentum transfer, we took the intermediate value $\theta_q = 80^\circ$. The total emission energy considered in our calculation was also chosen in the middle of the measured range: 10 eV per electron.

The cross sections, as defined by Eq. (13), are presented in Fig. 9. Our GSF calculation (contour plots, top panel) are compared with experimental data (middle panel). To appreciate the qualitative agreement between them, we present in the bottom panel a superposition of both results. In the small-q regime, the back-to-back configuration is not favored like the dipolar behavior observed with electron-impact collisions [14]. As the momentum transfer is increased, nondipolar terms become relevant: indeed, we observe in the calculated FDCS an important amount of back-to-back emission, and the binary and recoil peaks have very different shapes. The results show a strong, localized, binary peak; the recoil peak, in contrast, merges with the back-to-back one, forming a *wall* that has a dip in height precisely where the first-order Born symmetry axis crosses it. Unfortunately, the experimental detector range [11] precludes a comparison in the region where the recoil and back-to-back wall gains height.

An aspect that emerges from Fig. 9(b) is the small number of counts in the experiment. It does still allow for the visualization of some structures, but they are less clearly delimited than in previous electron-impact experiments from the same group [16,34,36]. This small number of counts, sadly, does not allow us to make a more detailed comparison. A higher impact count could result in more reliable and descriptive experimental cross sections, which in turn would call for a

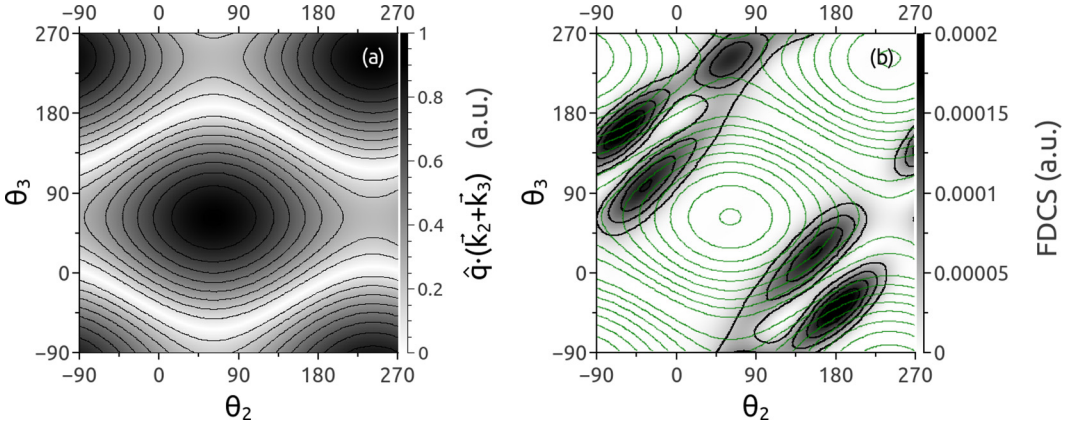

FIG. 8. (Color online) (a) $|\hat{\mathbf{q}} \cdot (\tilde{\mathbf{k}}_2 + \tilde{\mathbf{k}}_3)|$. (b) Same as Fig. 7(a), but superimposing the contours in (a) [in green (gray)].

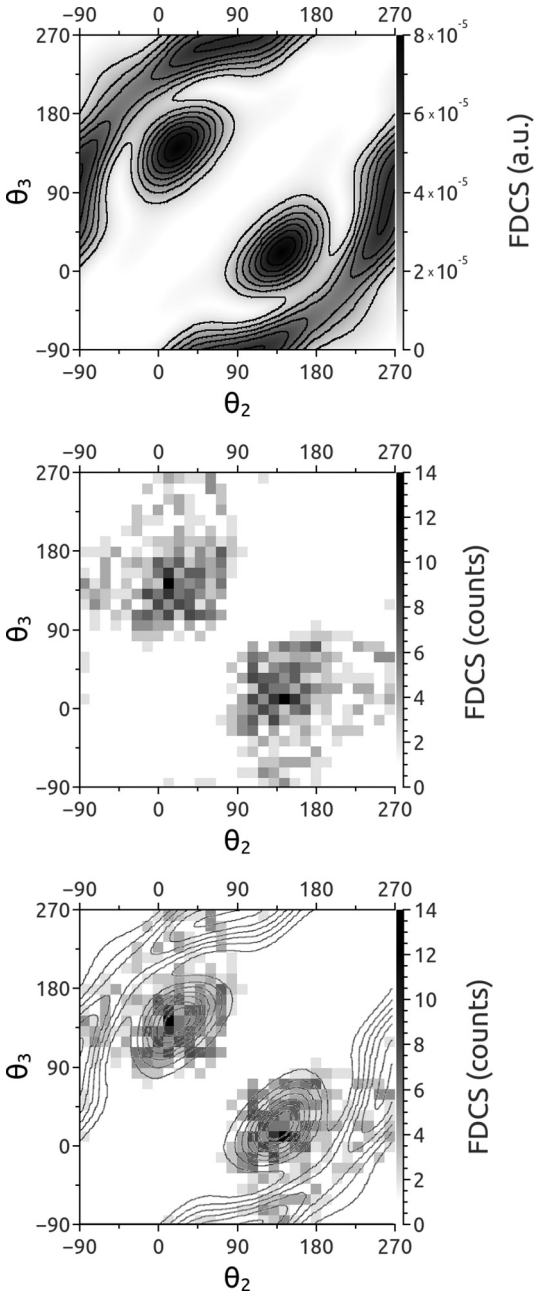

FIG. 9. Fully differential cross section for helium double ionization by protons impinging at 6 MeV, with two electrons ejected with the same energy. (top) Present GSF with momentum transfer $q = 1.65$, oriented at $\theta_q = 80^\circ$ and $E_2 = E_3 = 10$ eV. (middle) Relative experimental data [11] with a momentum transfer in the range $q = 1.4-2.0$ a.u., oriented in between $\theta_q = 75^\circ$ and 85° and $E_2 = E_3 < 25$ eV. (bottom) Superposition of the theoretical and experimental cross sections.

more sophisticated calculation with an actual integration on the energies and transferred momenta ranges, be it analytical or entirely numerical. This said, we may state that there is fair theory-experiment agreement in the cross-section shapes.

IV. SUMMARY

In the present contribution we have investigated FDCS for the double ionization of helium by protonic impact in different kinematical configurations. We tackled the problem within a first Born approximation frame regarding the projectile-target interaction and employing the generalized-Sturmian-function method to solve in a numerically exact way the resulting three-body continuum problem.

Our *ab initio* results allowed us to test the validity of approximate analytical double-continuum wave functions with effective charges or effective momenta. With the comparison in the explored kinematical conditions, we can state that (i) none of these schemes can provide an exact agreement with our calculations and (ii) of the two, the effective momentum approach can be deemed more physically plausible since it yielded FDCS which vary less abruptly with the ejection angles, similar to what was observed in our numerical results.

The EM3C approach has also been applied within a low-emission-energy regime [4]. Being slowly ejected, the electrons have time to interact with each other and with the core many times, corresponding to high orders in a multiple-scattering series [2]. These interactions are solved to every order by our *ab initio* GSF methodology. Although perturbative methods are normally considered not well suited to describe the dynamics of slowly ejected electrons, the EM3C model surprisingly managed to characterize the most dominant cross-section feature, namely, the recoil peak. While it still missed the binary and back-to-back contributions that show up in our GSF calculation in the $(3 + 3)$ eV regime, the study indicates that the EM3C provided an interesting step forwards for perturbative approaches.

The final results section was devoted to a theory-experiment FDCS comparison. We calculated GSF cross sections, attempting to replicate the relative experimental data of Fischer *et al.* [11], who registered low counting rates. Globally, we observed fair qualitative agreement, in particular with respect to two key features: the location of the maximum corresponding to the binary peak and the presence of a dip where the recoil peak was expected. There is also an experimental hint of a local peak in the cross section, corresponding to our theoretical back-to-back peak, but this falls outside of the detection angles for the cold-target recoil-ion momentum spectroscopy apparatus [11].

New fully differential experimental data, with fast incident protons, would be very welcome in order to validate the benchmark cross sections presented here. Furthermore, as was done with electron-impact ionization [13,15,16,37], the incidence energy could be lowered to quantify the appearance of second-order Born effects. We hope that our contribution will help with further theoretical developments in improving perturbation schemes.

ACKNOWLEDGMENTS

We thank Dr. S. D. López and Dr. D. Fischer for providing the results of their previous publications in tabular form. We acknowledge the support from PIP 201301/607 CONICET (Argentina), and one of the authors (G.G.) is also thankful for the support from PGI 24/F059 of the Universidad Nacional del Sur. We acknowledge the CNRS (PICS 06304) and CONICET (Project No. Dl 158114) for funding our French-Argentinean collaboration.

[1] L. Gulyás, A. Igarashi, and T. Kirchner, Phys. Rev. A **86**, 024701 (2012).
[2] J. Berakdar, A. Lahmam-Bennani, and C. Dal Cappello, Phys. Rep. **374**, 91 (2003).
[3] M. Schulz, M. F. Ciappina, T. Kirchner, D. Fischer, R. Moshammer, and J. Ullrich, Phys. Rev. A **79**, 042708 (2009).
[4] S. D. López, S. Otranto, and C. R. Garibotti, Phys. Rev. A **87**, 022705 (2013).
[5] M. B. Shah and H. B. Gilbody, J. Phys. B **18**, 899 (1985).
[6] L. H. Andersen, P. Hvelplund, H. Knudsen, S. P. Møller, K. Elsener, K. G. Rensfelt, and E. Uggerhøj, Phys. Rev. Lett. **57**, 2147 (1986).
[7] L. H. Andersen, P. Hvelplund, H. Knudsen, S. P. Møller, J. O. P. Pedersen, S. Tang-Petersen, E. Uggerhøj, K. Elsener, and E. Morenzoni, Phys. Rev. A **41**, 6536 (1990).
[8] M. Schulz, R. Moshammer, W. Schmitt, H. Kollmus, B. Feuerstein, R. Mann, S. Hagmann, and J. Ullrich, Phys. Rev. Lett. **84**, 863 (2000).
[9] M. Foster, J. Colgan, and M. S. Pindzola, Phys. Rev. Lett. **100**, 033201 (2008).
[10] X. Guan and K. Bartschat, Phys. Rev. Lett. **103**, 213201 (2009).
[11] D. Fischer, R. Moshammer, A. Dorn, J. R. Crespo López-Urrutia, B. Feuerstein, C. Höhr, C. D. Schröter, S. Hagmann, H. Kollmus, R. Mann *et al.*, Phys. Rev. Lett. **90**, 243201 (2003).
[12] S. D. López, C. R. Garibotti, and S. Otranto, Phys. Rev. A **83**, 062702 (2011).
[13] A. Kheifets, I. Bray, Lahmamm-Bennani, A. Duguet, and I. Taouil, J. Phys. B **32**, 5047 (1999).
[14] A. Lahmam-Bennani, I. Taouil, A. Duguet, M. Lecas, L. Avaldi, and J. Berakdar, Phys. Rev. A **59**, 3548 (1999).
[15] A. Lahmam-Bennani, A. Duguet, M. N. Gaboriaud, I. Taouil, M. Lecas, A. Kheifets, J. Berakdar, and C. D. Cappello, J. Phys. B **34**, 3073 (2001).
[16] A. Dorn, A. Kheifets, C. D. Schröter, B. Najjari, C. Höhr, R. Moshammer, and J. Ullrich, Phys. Rev. Lett. **86**, 3755 (2001).
[17] M. J. Ambrosio, F. D. Colavecchia, D. M. Mitnik, and G. Gasaneo, Phys. Rev. A **91**, 012704 (2015).
[18] M. J. Ambrosio, F. D. Colavecchia, G. Gasaneo, D. M. Mitnik, and L. U. Ancarani, J. Phys. B **48**, 055204 (2015).
[19] I. Bray, Phys. Rev. Lett. **89**, 273201 (2002).
[20] C. W. McCurdy, M. Baertschy, and T. N. Rescigno, J. Phys. B **37**, R137 (2004).
[21] M. Silenou Mengoue, M. G. Kwato Njock, B. Piraux, Y. V. Popov, and S. A. Zaytsev, Phys. Rev. A **83**, 052708 (2011).
[22] G. Gasaneo, L. U. Ancarani, D. M. Mitnik, J. M. Randazzo, A. L. Frapiccini, and F. D. Colavecchia, Adv. Quantum Chem. **67**, 153 (2013).
[23] C. R. Garibotti and J. E. Miraglia, Phys. Rev. A **21**, 572 (1980).
[24] J. S. B. M Brauner and H. Klar, J. Phys. B **22**, 2265 (1989).
[25] D. M. Mitnik, F. D. Colavecchia, G. Gasaneo, and J. M. Randazzo, Comput. Phys. Commun. **182**, 1145 (2011).
[26] J. M. Randazzo, D. M. Mitnik, G. Gasaneo, L. U. Ancarani, and F. Colavecchia, Eur. J. Phys. D **69**, 189 (2015).
[27] A. S. Kheifets, I. Bray, J. Berakdar, and C. Dal Cappello, J. Phys. B **35**, L15 (2002).
[28] S. D. López, S. Otranto, and C. R. Garibotti, Phys. Rev. A **89**, 062709 (2014).
[29] M. F. Ciappina, T. Kirchner, and M. Schulz, Phys. Rev. A **84**, 034701 (2011).
[30] G. Gasaneo, D. M. Mitnik, J. M. Randazzo, L. U. Ancarani, and F. D. Colavecchia, Phys. Rev. A **87**, 042707 (2013).
[31] A. S. Kadyrov, A. M. Mukhamedzhanov, A. T. Stelbovics, I. Bray, and F. Pirlepesov, Phys. Rev. A **68**, 022703 (2003).
[32] J. M. Randazzo, A. L. Frapiccini, F. D. Colavecchia, and G. Gasaneo, Phys. Rev. A **79**, 022507 (2009).
[33] J. M. Randazzo, A. L. Frapiccini, F. D. Colavecchia, and G. Gasaneo, Int. J. Quantum Chem. **109**, 125 (2009).
[34] A. Dorn, A. Kheifets, C. D. Schröter, B. Najjari, C. Höhr, R. Moshammer, and J. Ullrich, Phys. Rev. A **65**, 032709 (2002).
[35] E. O. Alt and A. M. Mukhamedzhanov, Phys. Rev. A **47**, 2004 (1993).
[36] A. Dorn, G. Sakhelashvili, C. Höhr, A. Kheifets, J. Lower, B. Najjari, C. Schröter, R. Moshammer, and J. Ullrich, in Electron and Photon Impact Ionization and Related Topics, IOP Conference Proceedings Vol. 172 (IOP Publishing, Bristol, UK, 2003), p. 41.
[37] A. Lahmam-Bennani, E. M. S. Casagrande, A. Naja, C. D. Cappello, and P. Bolognesi, J. Phys. B **43**, 105201 (2010).